29th International Conference
ENGINEERING MECHANICS 2023
Milovy, Czech Republic, May 9 – 11, 2023

FINITE ELEMENT MODAL ANALYSIS OF A SILICONE VOCAL FOLD FILLED WITH FLUID

Hájek P.*, Radolf V., Horáček J.***, Švec J. G.†**

Abstract: *A three dimensional (3D) finite element (FE) model of a silicone vocal fold (VF) filled with fluid is presented here. The silicone part of the model is based on partial differential equations of the continuum mechanics and consider large deformations. The fluid domain encapsulated in the silicone VF is defined semi-analytically as a lumped-element model describing the fluid in hydrostatic conditions. The elongated and pressurized silicone VF was subjected to perturbed modal analysis. Results showed that the choice of the fluid inside the VF substantially influences the natural frequencies. Namely, the water-filling lowers the natural frequencies approximately by half over the air-filling. Besides, the procedure of reverse engineering for obtaining the geometry of the VF from already 3D-printed mold is introduced.*

Keywords: Perturbed Modal Analysis, Finite Element Method, Vocal Folds, Reverse Engineering, Biomechanics of Voice.

1. Introduction

Human phonation is a very complex phenomenon. Strong and non-linear interactions occur among all three fields involved in the phonation (Titze, 2008; Švec et al., 2021): structural mechanics, fluid mechanics and acoustics. In order to simulate such a phenomenon, many approaches can be found in the literature – from computational modeling, to experiments on cadavers or on artificial models. The latter approach is especially hard to tune.

The human phonation mainly depends on the combination of vocal fold (VF) properties, VF activation and an initial VF position, subglottal pressure and inertia of surrounding air column. The subglottal pressure is reliant on power of the human lungs; activation and initial position of the VFs is controlled by laryngeal muscles, and the posture of the cartilages and the VF properties depend on the incorporated layers and material of these layers (Isshiki, 1980). All these conditions must be harmonized together and should be included in experimental models. Correct tuning of the material properties of the VF layers in such models is substantial to achieve sustained oscillation (Zhang et al., 2009). A reasonable indicator for proper tuning of the layered VF in the experimental setup can be a modal analysis.

2. Methods

2.1. Geometry of the Vocal Fold

Shape of the VF was extracted from the 3D-printed mold by means of reverse engineering. Original contour of the 3D-printed mold (Vampola et al., 2016a) was acquired from computer tomography (CT) scans. The mold comprises exterior surface of the VF, epithelium and muscle.

* Ing. Petr Hájek, Ph.D.: Institute of Solid Mechanics, Mechatronics and Biomechanics, Brno University of Technology, Technická 2896/2; 616 69, Brno; CZ; Voice Research Laboratory, Department of Experimental Physics, Palacký University Olomouc; 17. listopadu 1192/12; 779 00, Olomouc; CZ, hajek.p@fme.vutbr.cz
** Ing. Vojtěch Radolf, Ph.D.: Institute of Thermomechanics of the Czech Academy of Sciences; Dolejškova 1402/5; 182 00, Prague; CZ, radolf@it.cas.cz
*** Ing. Jaromír Horáček, DrSc.: Institute of Thermomechanics of the Czech Academy of Sciences; Dolejškova 1402/5; 182 00, Prague; CZ, jaromirh@it.cas.cz
† doc. RNDr. Jan G. Švec, Ph.D. et Ph.D.: Voice Research Laboratory, Department of Experimental Physics, Palacký University Olomouc; 17. listopadu 1192/12; 779 00, Olomouc; CZ, jan.svec@upol.cz

ISSN: 1805-8256, doi: 10.21495/em2023-87

The 3D-printed mold was scanned using the optical scanner Shining 3D® EinScan SE with a spatial resolution of $0.1\,\mathrm{mm}$. The produced STL file was adjusted in GOM Inspect software to extract a smooth part of the VF surface. The surface was read into Python 3.8.5 using the `numpy-stl` package, divided into points and then cut to obtain a representative contour of the VF surface (see fig. 1a). The contour was exported as a STEP file using the `pythonOCC` package, which is a Python wrapper for the OpenCASCADE Technology written in C++. The final shape of the VF was reconstructed using an interpolation spline tool in Autodesk® Inventor® 2023. The reconstructed geometry is in fig. 1 together with overall dimensions. Mutual position of the parts of the original mold (exterior surface, epithelium and muscle) was measured on the optical scan and checked with a caliper.

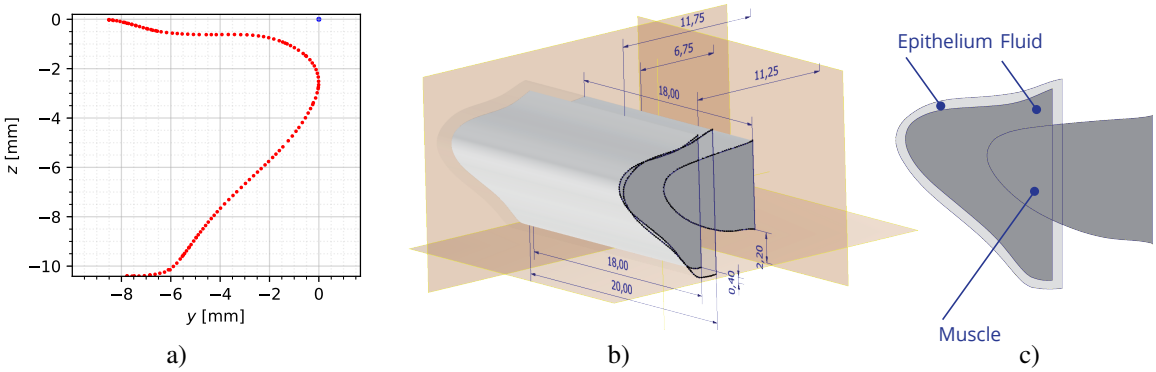

a) b) c)

Fig. 1. Stages of the VF geometry reconstruction: a) points of one slice of the representative VF contour, b) the geometry in $[\mathrm{mm}]$ of the VF extracted from the 3D-printed mold and c) side view of the complete geometry with layers. Note, that the majority of the muscle was cut out at the vertical plane of the exterior VF surface.

2.2. Model of Material

The epithelium of the VF and the muscle (see fig. 1c) of the molded synthetic model was made from the Smooth-On Ecoflex™ 00–10 silicone (see fig. 2a). Although silicones show rather hyperelastic behavior, the Hookean material model was used in the numerical model because they evince linear behavior approximately to 10% strain (Thomson, 2004). The material parameters were obtained from a product sheet of the silicone and from Thomson (2004): Young's modulus $E_s = 60\,\mathrm{kPa}$, density $\rho_s = 1040\,\mathrm{kg}\cdot\mathrm{m}^{-3}$, Poisson's ratio $\mu_s = 0.45$ and coefficients of proportional damping $\alpha_s = 14.4\,\mathrm{s}^{-1}$ and $\beta_s = 0.00043\,\mathrm{s}$.

An empty space between the epithelium and the muscle (see fig. 1c) or 2c) was filled with fluid in the synthetic model: either air or water. In the numerical model, air (denoted by the subscript a) was modeled as compressible ideal gas at room temperature with density $\rho_a = 1.1972\,\mathrm{kg}\cdot\mathrm{m}^{-3}$ (Tsilingiris, 2018). Water (denoted by the subscript w) was assumed to be incompressible at the same conditions with bulk modulus $K_w = 2.1\,\mathrm{GPa}$, coefficient of thermal expansion $\alpha_w = 2.07{\cdot}10^{-4}\,\mathrm{K}^{-1}$ and density $\rho_w = 1020\,\mathrm{kg}\cdot\mathrm{m}^{-3}$ (Vampola et al., 2016b).

2.3. Finite Element Model

A three dimensional (3D) finite element (FE) model was created in ANSYS® Mechanical APDL™, Release 2021 R2 (see fig. 2b)–d) and only the oscillating part of the physical VF was modeled (see fig. 2a). The silicone part (epithelium and muscle, recall fig. 1c) was divided into 8312 quadratic structural elements `SOLID186` and 43383 nodes with three degrees of freedom (DOFs, displacements in axes x, y and z). The fluid part (fig. 1c) was modeled semi-analytically with one master node (see fig. 2d) inside the fluid domain with one DOF (hydrostatic pressure) and with 3624 surface elements `HSFLD242` with 10875 nodes, which are lining the empty space inside the VF – sloshing effects were not included. The master node controls the fluid properties and the hydrostatic pressure, which is then prescribed to the surface elements together with mass corresponding to the volume of the encapsulated fluid.

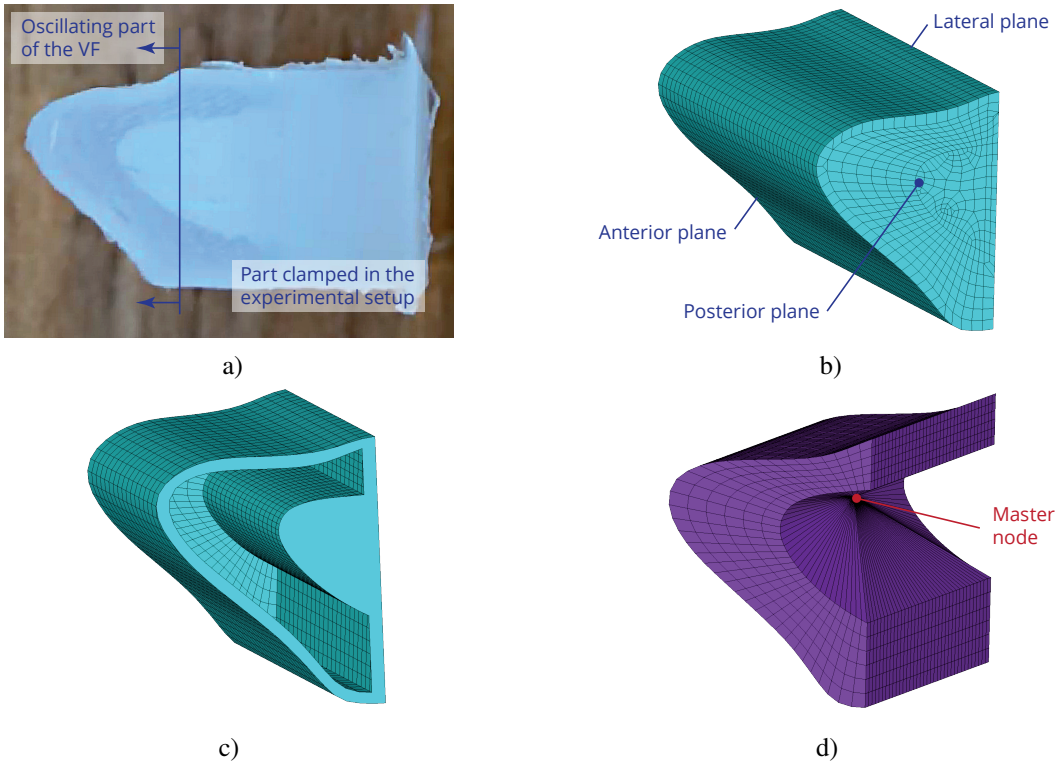

Fig. 2. Models: a) the silicone model, b) the complete finite element model, c) the empty space inside the VF prepared for the fluid elements and d) the fluid domain with the master node.

2.4. Algorithm and Boundary Conditions

The computational algorithm had two stages: at first, non-linear structural analysis was performed, then a perturbed modal analysis was computed. The perturbed analysis is a linear analysis on top of the (generally) non-linear analysis from which the resulting stiffness matrix is passed to the perturbed analysis.

Boundary conditions were adopted from the physical setup (Horáček et al., 2019) for both analyses. During the structural analysis, large deformations were taken into account and the VF was elongated in anteroposterior direction. Displacement of $2\,\mathrm{mm}$ was prescribed on the posterior plane while the anterior plane was clamped. Displacement on the lateral plane was set free in anteroposterior direction, other DOFs were fixed. The hydrostatic pressure of $500\,\mathrm{Pa}$ was prescribed inside the VF, so the fluid stayed in hydrostatic conditions through the whole structural analysis. The anterior, posterior and lateral planes were fixed in the elongated and inflated shape through the perturbed modal analysis.

3. Results and Discussion

The first two mode shapes with corresponding natural frequencies are shown in fig. 3 for the VF filled with air (top panel) and water (bottom panel). Adding the water inside the VF lowers the natural frequencies approximately to the half, so it can be expected that the water can also lower the vibration frequency of the physical VF.

The mode shapes in the air-filled VF are related to the movement of the epithelium, which is more or less in the craniocaudal direction. By contrast, the water-filled VF tends to vibrate more in the apex of the VF in the mediolateral direction. In both cases, the first two mode shapes had maximal amplitudes at the middle of the VF and are expected to take part in the travelling waves on the VF surface.

4. Conclusion

FE model of a VF filled with pressurized fluid was created. Results of the modal analysis showed that filling of the VF with different fluids can significantly affect the natural frequencies and thus the vibration frequency of the self-sustained oscillation of the VF. Also the pretension of the VF in the anteroposterior direction and the inner pressure is expected to influence the natural frequencies and therefore the VF

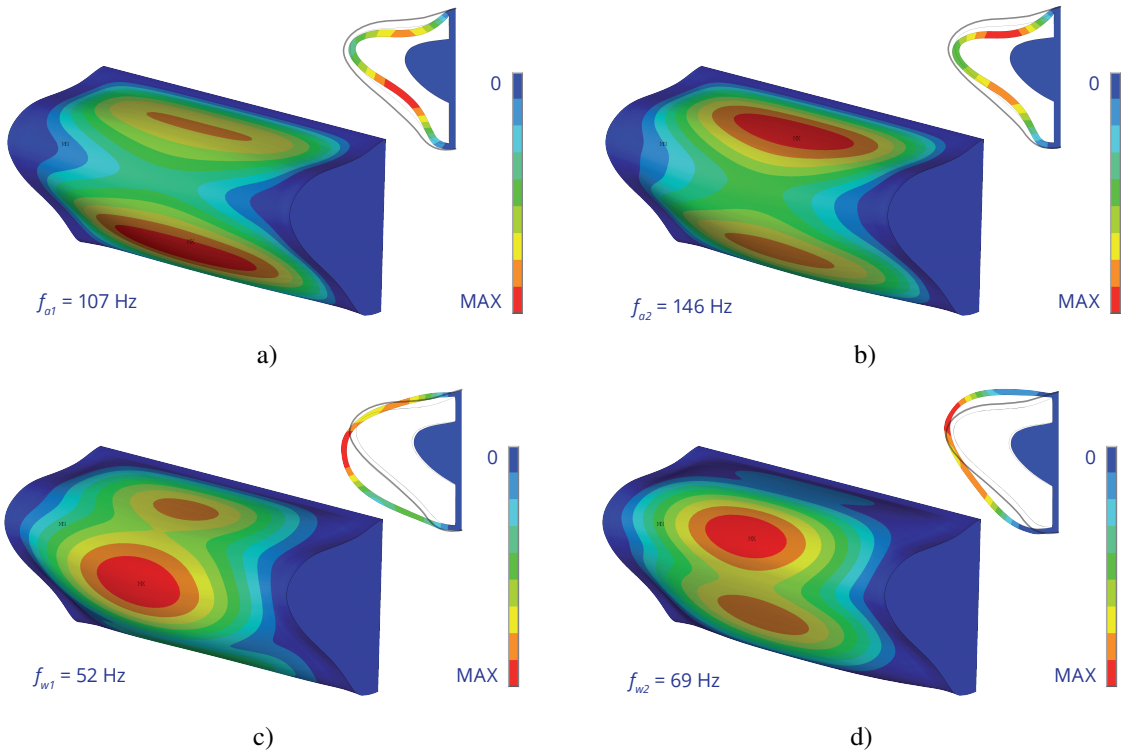

Fig. 3. Mode shapes of the VF filled with air: a) 1st mode, 107 Hz, b) 2nd mode, 146 Hz. VF filled with water: c) 1st mode, 52 Hz, d) 2nd mode, 69 Hz. The small views in the top-right corner of each panel are coronal sections in the middle of the VF.

oscillation. The boundary conditions of the presented numerical model were tuned to correspond to the conditions during the physical experiment. Previous measurements showed that the air-filled VFs are vibrating between ca. 100 and 200 Hz during the experiment and the water-filled VFs between ca. 60 and 120 Hz (Horáček et al., 2019), which is in good agreement with the presented model. This model could be used for fine tuning of the vibrating VFs.

References

Horáček, J., Radolf, V., and Laukkanen, A.-M. (2019) Experimental and Computational Modeling of the Effects of Voice Therapy Using Tubes. *Journal of Speech, Language, and Hearing Research*, 62, 7, pp. 2227–2244.

Isshiki, N. (1980) Recent Advances in Phonosurgery. *Folia Phoniatrica et Logopaedica*, 32, 2, pp. 119–154.

Švec, J. G., Schutte, H. K., Chen, C. J., and Titze, I. R. (2021) Integrative Insights into the Myoelastic-Aerodynamic Theory and Acoustics of Phonation. Scientific Tribute to Donald G. Miller. *Journal of voice*, pp. S0892–1997(21)00055–2, doi: 10.1016/j.jvoice.2021.01.023.

Thomson, S. L. (2004) *Fluid-Structure Interactions within the Human Larynx*. PhD thesis, Purdue University.

Titze, I. R. (2008) Nonlinear source–filter coupling in phonation: Theory. *Journal of the Acoustical Society of America*, 123, 5, pp. 2733–2749.

Tsilingiris, P. T. (2018) Review and critical comparative evaluation of moist air thermophysical properties at the temperature range between 0 and 100°C for Engineering Calculations. *Renewable and Sustainable Energy Reviews*, 83, pp. 50–63.

Vampola, T., Horáček, J., Dušková-Smrčková, M., Köhler, J., and Klepáček, I. (2016a) A Vocal Cord Substitution and a Method of Tuning the Vocal Cord Substitution. European Patent Application EP 3 072477 A1, date of publication: 28.09.2016, Bulletin 2016/39.

Vampola, T., Horáček, J., and Klepáček, I. (2016b) Computer simulation of mucosal waves on vibrating human vocal folds. *Biocybernetics and Biomedical Engineering*, 36, 3, pp. 451–465.

Zhang, Z., Neubauer, J., and Berry, D. A. (2009) Influence of vocal fold stiffness and acoustic loading on flow-induced vibration of a single-layer vocal fold model. *Journal of Sound and Vibration*, 322, 1, pp. 299–313.